

$Y(4260)$ on the lattice

Ting-Wai Chiu¹, Tung-Han Hsieh²

¹*Department of Physics, National Taiwan University,
Taipei, 10617, Taiwan*

²*Physics Section, Commission of General Education,
National United University, Miao-Li, 36003, Taiwan*

(TWQCD Collaboration)

Abstract

We investigate the mass spectra of closed-charm mesons with $J^{PC} = 1^{--}$, for hybrid charmonium, molecules, and diquark-antidiquark operators, in quenched lattice QCD with exact chiral symmetry. For two lattice volumes $24^3 \times 48$ and $20^3 \times 40$, each of 100 gauge configurations generated with single-plaquette action at $\beta = 6.1$, we compute point-to-point quark propagators and measure the time-correlation functions of these exotic meson operators. For the molecular operator $\{(\bar{\mathbf{q}}\gamma_5\gamma_i\mathbf{c})(\bar{\mathbf{c}}\gamma_5\mathbf{q}) - (\bar{\mathbf{c}}\gamma_5\gamma_i\mathbf{q})(\bar{\mathbf{q}}\gamma_5\mathbf{c})\}$, it detects a resonance with mass around 4238 ± 31 MeV, which is naturally identified with $Y(4260)$. Further, for any molecular and diquark-antidiquark operator, it detects heavier exotic charmed mesons, with $(\mathbf{c}\bar{\mathbf{s}}\bar{\mathbf{c}})$ around 4450 ± 100 MeV, and $(\mathbf{c}\bar{\mathbf{c}}\bar{\mathbf{c}})$ around 6400 ± 50 MeV.

PACS numbers: 11.15.Ha, 11.30.Rd, 12.38.Gc

Keywords: Lattice QCD, Exact Chiral Symmetry, Exotic mesons, Charmed Mesons, Diquarks

1 Introduction

Recently, a new state $Y(4260)$ with a mass of $4259(8)(4)$ MeV and a width $88(23)(5)$ MeV, in association with an initial state radiation photon, has been observed by BaBar collaboration in e^-e^+ annihilation [1]. This immediately implies that its $J^{PC} = 1^{--}$. From the experimental and theoretical spectrum of $(c\bar{c})$ states, $Y(4260)$ can hardly be interpreted as one of the radial and/or orbital excitations of $(c\bar{c})$. Thus it is most likely an exotic (non- $q\bar{q}$) meson.

So far, theoretical models to understand $Y(4260)$ are: (i) hybrid charmonium $\bar{c}cg$ [2, 3], (ii) P-wave excitation of the diquark-antidiquark $[\mathbf{cs}][\bar{\mathbf{c}}\bar{\mathbf{s}}]$ [4]; and (iii) molecule composed of 2 mesons, e.g., $\rho\chi_{c1}$ [5].

Now the important question is whether there is a resonance around 4260 MeV with $J^{PC} = 1^{--}$, in the spectrum of QCD. In this paper, we investigate the mass spectra of several interpolating operators whose lowest-lying states have $J^{PC} = 1^{--}$, in lattice QCD with exact chiral symmetry [6, 7, 8, 9, 10]. For two lattice volumes $24^3 \times 48$ and $20^3 \times 40$, each of 100 gauge configurations generated with single-plaquette action at $\beta = 6.1$, we compute point-to-point quark propagators for 30 quark masses in the range $0.03 \leq m_q a \leq 0.80$, and measure the time-correlation functions of the exotic meson operators which can overlap with $Y(4260)$. The inverse lattice spacing a^{-1} is determined with the experimental input of f_π , while the strange quark bare mass $m_s a = 0.08$, and the charm quark bare mass $m_c a = 0.80$ are fixed such that the masses of the corresponding vector mesons are in good agreement with $\phi(1020)$ and $J/\psi(3097)$ respectively [11]. Our scheme of computing quark propagators has been outlined in [12].

Note that we are working in the quenched approximation which in principle is unphysical. However, our previous results on charmed baryon masses, and also charmed meson masses and decay constants (theoretical predictions) [11] turn out to be in good agreement with the experimental values. This seems to suggest that it is plausible to use the quenched lattice QCD with exact chiral symmetry to investigate the mass spectra of the charmed meson operators constructed in this paper, as a first step toward the unquenched calculations. The systematic error due to quenching can only be determined after we can repeat the same calculation with unquenched gauge configurations. However, the Monte Carlo simulation of unquenched gauge configurations for lattice QCD with exact chiral symmetry, on the lattices $20^3 \times 40$ and $24^3 \times 48$ at $\beta = 6.1$, still remains a great challenge to the lattice community. Thus, in this paper, we proceed with the quenched approximation, assuming that the quenching error does not change our conclusions dramatically, in view of the good agreement between our previous quenched mass spectra of charmed hadrons [11] and the experimental values.

2 The Hybrid Charmonium $\bar{c}c g$

The local interpolating operators for hybrid charmonium with $J^{PC} = 1^{--}$ can be constructed as $\bar{c}F_{4i}c$, $\epsilon_{ijk}\bar{c}\gamma_5 F_{jk}c$, and $\epsilon_{ijk}\bar{c}\gamma_4\gamma_5 F_{jk}c$. Here the matrix-valued gluon field tensor $F_{\mu\nu}(x)$ can be obtained from the four plaquettes surrounding x on the $(\hat{\mu}, \hat{\nu})$ plane, i.e.,

$$ga^2 F_{\mu\nu}(x) \simeq \frac{1}{8i} [P_{\mu\nu}(x) + P_{\mu\nu}(x - \hat{\mu}) + P_{\mu\nu}(x - \hat{\nu}) + P_{\mu\nu}(x - \hat{\mu} - \hat{\nu}) - P_{\mu\nu}^\dagger(x) - P_{\mu\nu}^\dagger(x - \hat{\mu}) - P_{\mu\nu}^\dagger(x - \hat{\nu}) - P_{\mu\nu}^\dagger(x - \hat{\mu} - \hat{\nu})]$$

where

$$P_{\mu\nu}(x) = U_\mu(x)U_\nu(x + \hat{\mu})U_\mu^\dagger(x + \hat{\nu})U_\nu^\dagger(x) .$$

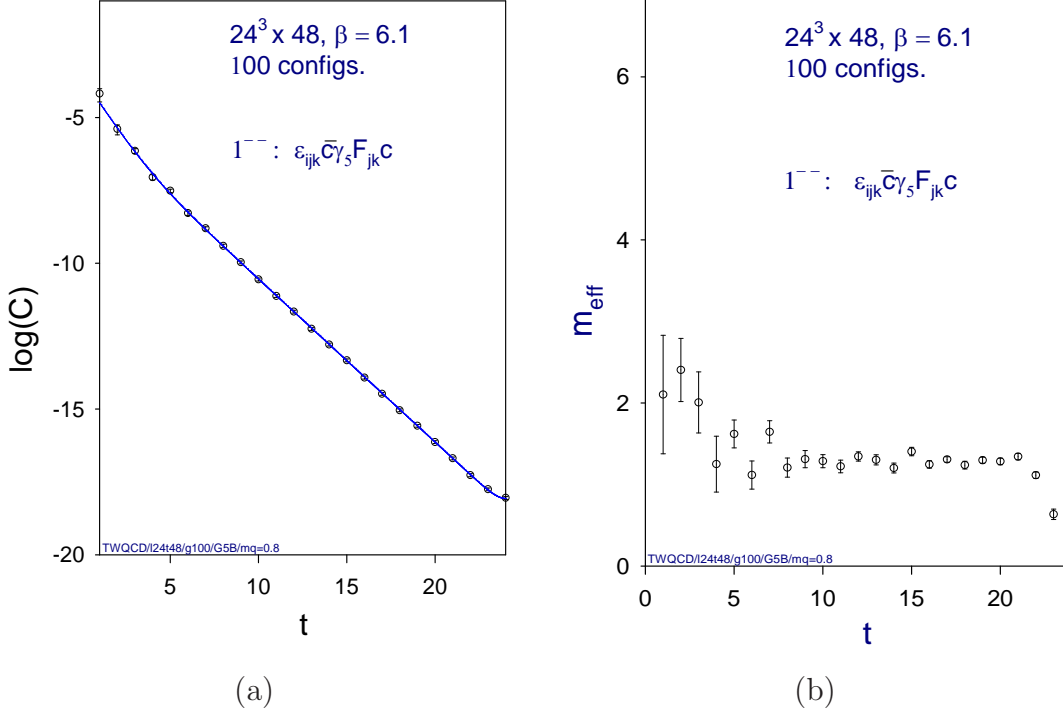


Figure 1: (a) The time-correlation function $C(t)$ of the hybrid meson operator $\epsilon_{ijk}\bar{c}\gamma_5 F_{jk}c$ with $J^{PC} = 1^{--}$, on the $24^3 \times 48$ lattice at $\beta = 6.1$. The solid line is the double hyperbolic-cosine fit for $t \in [1, 24]$. (b) The effective mass $M_{\text{eff}}(t) = \ln[C(t)/C(t+1)]$ of $C(t)$ in Fig. 1a.

In Fig. 1, the time-correlation function $C(t)$ of the hybrid charmonium operator $\epsilon_{ijk}\bar{c}\gamma_5 F_{jk}c$ is plotted, together with the effective mass $\ln[C(t)/C(t+1)]$, for 100 gauge configurations generated with single-plaquette action on

$24^3 \times 48$ at $\beta = 6.1$. Here $C(t)$ has been averaged over $i = 1, 2, 3$, where in each case, the “forward-propagator” $C_i(t)$ and “backward-propagator” $C_i(T - t)$ are averaged to increase the statistics. The same strategy is applied to all time-correlation functions in this paper. The solid line in (a) is the double hyperbolic-cosine fit

$$W_1 \left(e^{-m_1 at} + e^{-m_1 a(T-t)} \right) + W_2 \left(e^{-m_2 at} + e^{-m_2 a(T-t)} \right)$$

for $t \in [1, 24]$. It gives $m_1 = 2977(28)$ MeV and $m_2 = 4501(178)$ MeV with $\chi^2/d.o.f. = 0.95$. In this paper, we have adopted the procedure outlined in Ref. [13] to perform our data fitting and error estimation. Now we identify the lowest-lying state with J/ψ , since the hybrid charmonium operator with 1^{--} also overlaps with J/ψ . Then the first excited state with mass 4501(178) MeV is identified with the lowest-lying hybrid charmonium with 1^{--} . Note that the error of the mass of the first excited state is relatively large, since it is obtained by double hyperbolic-cosine fit. Evidently the mass of the lowest-lying hybrid charmonium state with 1^{--} is higher than 4260 MeV. Thus it is unlikely to be identified with $Y(4260)$, even though we could not rule out such a possibility, due to the large error bar. Nevertheless, we will report a more precise determination of the mass of the hybrid charmonium with 1^{--} in a future publication.

3 The Molecular Operators

In this section, we construct three molecular operators with quark content $(\mathbf{c}\mathbf{q}\bar{\mathbf{c}}\bar{\mathbf{q}})$ such that the lowest-lying state of each operator has $J^{PC} = 1^{--}$. Then we compute the time correlation function of each operator, and extract the mass of its lowest-lying state. Explicitly, these molecular operators are:

$$M_1 = \frac{1}{\sqrt{2}} \{ (\bar{\mathbf{q}}\gamma_i\mathbf{c})(\bar{\mathbf{c}}\mathbf{q}) + (\bar{\mathbf{c}}\gamma_i\mathbf{q})(\bar{\mathbf{q}}\mathbf{c}) \} \quad (1)$$

$$M_2 = (\bar{\mathbf{c}}\gamma_i\mathbf{c})(\bar{\mathbf{q}}\mathbf{q}) \quad (2)$$

$$M_3 = \frac{1}{\sqrt{2}} \{ (\bar{\mathbf{q}}\gamma_5\gamma_i\mathbf{c})(\bar{\mathbf{c}}\gamma_5\mathbf{q}) - (\bar{\mathbf{c}}\gamma_5\gamma_i\mathbf{q})(\bar{\mathbf{q}}\gamma_5\mathbf{c}) \} \quad (3)$$

The time-correlation function¹

$$C_M(t) = \sum_{\vec{x}} \langle M(\vec{x}, t) M^\dagger(\vec{0}, 0) \rangle$$

is measured for each gauge configuration, and its average over all gauge configurations is fitted to the usual formula

$$\frac{Z}{2ma} [e^{-mat} + e^{-ma(T-t)}]$$

¹Here we have neglected the $\mathbf{c}\bar{\mathbf{c}}$ and $\mathbf{q}\bar{\mathbf{q}}$ annihilation diagrams such that $C(t)$ does not overlap with any conventional meson ($\mathbf{c}\bar{\mathbf{c}}$ or $\mathbf{q}\bar{\mathbf{q}}$) states.

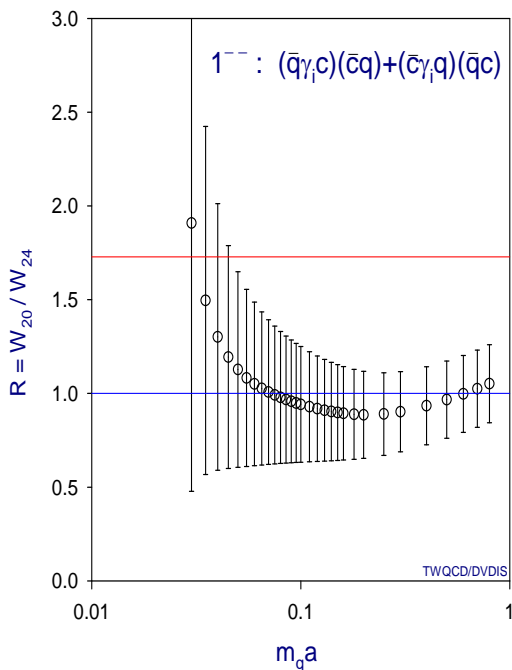


Figure 2: The ratio of spectral weights of the lowest-lying state of the molecular operator M_1 , for $20^3 \times 40$ and $24^3 \times 48$ lattices at $\beta = 6.1$. The upper-horizontal line $R = (24/20)^3 = 1.728$, is the signature of 2-particle scattering state, while the lower-horizontal line $R = 1.0$ is the signature of a resonance.

to extract the mass ma of the lowest-lying state and its spectral weight

$$W = \frac{Z}{2ma} .$$

Theoretically, if this state is a genuine resonance, then its mass ma and spectral weight W should be almost constant for any lattices with the same lattice spacing. On the other hand, if it is a 2-particle scattering state, then its mass ma is sensitive to the lattice volume, and its spectral weight is inversely proportional to the spatial volume for lattices with the same lattice spacing. In the following, we shall use the ratio of the spectral weights on two spatial volumes 20^3 and 24^3 with the same lattice spacing ($\beta = 6.1$) to discriminate whether any hadronic state under investigation is a resonance or not.

In Fig. 2, the ratio ($R = W_{20}/W_{24}$) of spectral weights of the lowest-lying state extracted from the time-correlation function of M_1 on the $20^3 \times 40$ and $24^3 \times 48$ lattices is plotted versus the quark mass $m_q a \in [0.03, 0.8]$. Evidently, $R \simeq 1.0$ for $m_q a > 0.05$, which implies that there exist 1^{--} resonances with quark contents $(\mathbf{cc}\bar{c}\bar{c})$ and $(\mathbf{cs}\bar{c}\bar{s})$. On the other hand, as $m_q \rightarrow m_u$, R begins to deviate from 1.0 with large error. We suspect that this might be due to quenching artifacts as $m_q \rightarrow m_u$, mostly from the scalar meson component

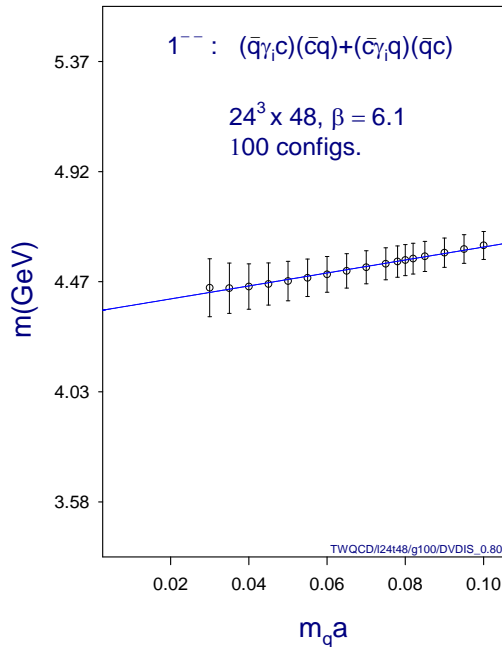


Figure 3: The mass of the lowest-lying state of M_1 versus the quark mass $m_q a$, on the $24^3 \times 48$ lattice at $\beta = 6.1$. The solid line is the linear fit with $\chi^2/d.o.f. = 0.34$.

$(\bar{c}q)$ or $(\bar{q}c)$ in the molecular operator M_1 . Thus R could be consistent with 1.0 if one incorporates internal quark loops, with higher statistics and larger volumes. If this is the case, a resonance might also exist for $\mathbf{q} = \mathbf{u}$. In the following, we assume this is the case, and chirally extrapolate the mass of the molecule M_1 to the limit $m_q \rightarrow m_u$.

In Fig. 3, the mass of the lowest-lying state extracted from the molecular operator M_1 is plotted versus $m_q a$, which can be fitted by the linear function $m = c_0 + c_1 m_q$ with $\chi^2/d.o.f. = 0.34$. In the limit $m_q \rightarrow m_u$, it gives $m = 4350(69)$ MeV which is compatible with the mass of $Y(4260)$.

For $m_q = m_s$, and $m_q = m_c$, the time-correlation functions and effective masses of M_1 are plotted in Fig. 4 and Fig. 5 respectively. The masses of the lowest-lying states are: $m[(\bar{s}\gamma_i c)(\bar{c}s) + (\bar{c}\gamma_i s)(\bar{s}c)] = 4546(30)$ MeV with $\chi^2/d.o.f. = 0.97$, and $m[(\bar{c}\gamma_i c)(\bar{c}c)] = 6411(25)$ MeV with $\chi^2/d.o.f. = 0.61$.

Next we turn to the molecular operator M_2 . Obviously, it must suffer severely from the quenched artifacts as $m_q \rightarrow m_u$, due to the presence of the scalar meson operator $(\bar{q}q)$. Thus, we observe that in the limit $m_q \rightarrow m_u$, the time-correlation function becomes very noisy, and we could not obtain any reliable results of its masses and spectral weights. However, at $m_q = m_s = 0.08a^{-1}$, we can still extract its mass and spectral weight. For the $24^3 \times 48$

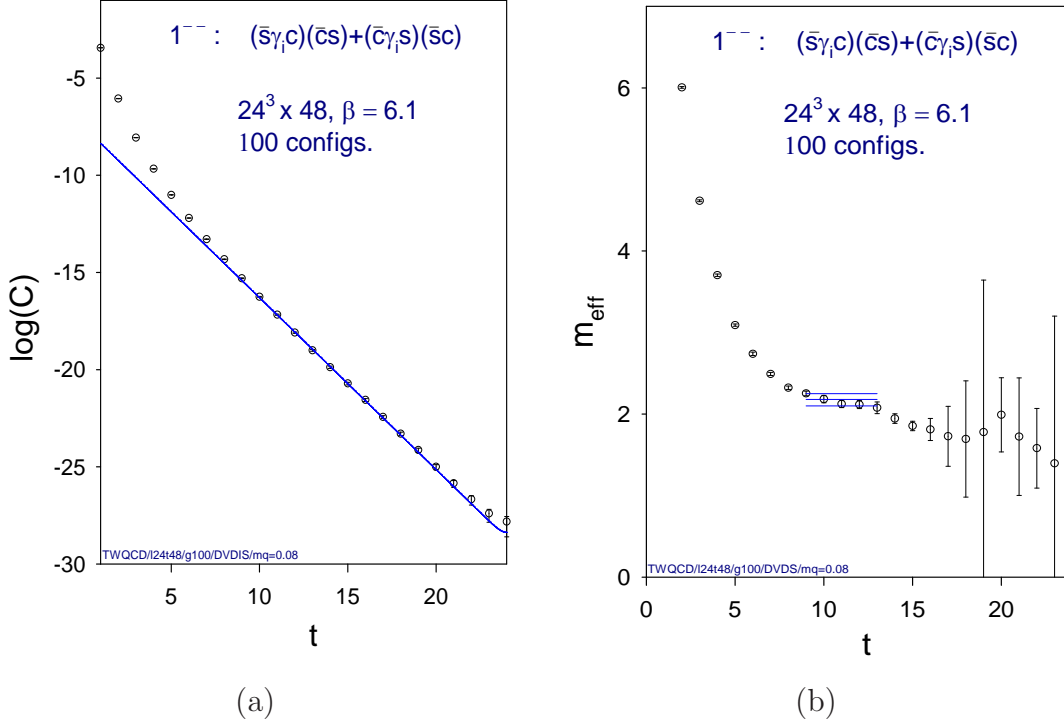


Figure 4: (a) The time-correlation function $C(t)$ of the lowest-lying state of M_1 for $m_q = m_s = 0.08a^{-1}$, on the $24^3 \times 48$ lattice at $\beta = 6.1$. The solid line is the hyperbolic-cosine fit for $t \in [9, 13]$ with $\chi^2/d.o.f. = 0.97$. (b) The effective mass $M_{eff}(t) = \ln[C(t)/C(t+1)]$ of $C(t)$ in Fig. 4a.

lattice (Fig. 6), the mass and spectral weight are: $m = 4581(96)$ MeV, and $W = 0.71(41) \times 10^{-7}$; while for the $20^3 \times 40$ lattice, $m = 4637(156)$ MeV, and $W = 0.92(80) \times 10^{-7}$. Thus the molecular operator $(\bar{\mathbf{c}}\gamma_i\mathbf{c})(\bar{\mathbf{s}}\mathbf{s})$ seems to detect a resonance with mass $4581(96)$ MeV (Fig. 6), which is compatible to that obtained from M_1 with $m_q = m_s$ (Fig. 4).

Next we consider the molecular operator M_3 . It is expected to suffer quenched artifacts less than those of M_1 and M_2 , since it is composed of a pseudoscalar meson operator $(\bar{\mathbf{c}}\gamma_5\mathbf{q})$ times a pseudovector meson operator $(\bar{\mathbf{q}}\gamma_5\gamma_i\mathbf{c})$, without any scalar meson operators like $(\bar{\mathbf{q}}\mathbf{q})$ or $(\bar{\mathbf{c}}\mathbf{q})$. In Fig. 7, the ratio ($R = W_{20}/W_{24}$) of spectral weights of the lowest-lying state extracted from the time-correlation function of M_3 on the $20^3 \times 40$ and $24^3 \times 48$ lattices is plotted versus the quark mass $m_q a \in [0.03, 0.8]$. Evidently, $R \simeq 1.0$ for the entire range of quark masses, which implies that there exist resonances with quark contents $(\mathbf{c}\bar{\mathbf{c}}\bar{\mathbf{c}})$, $(\mathbf{c}\bar{\mathbf{s}}\bar{\mathbf{s}})$, and $(\mathbf{c}\bar{\mathbf{u}}\bar{\mathbf{u}})$, even though R slightly deviates from one at small quark masses.

In Fig. 8, the mass of the lowest-lying state extracted from the molecular operator M_3 is plotted versus $m_q a$, which can be fitted by the linear function

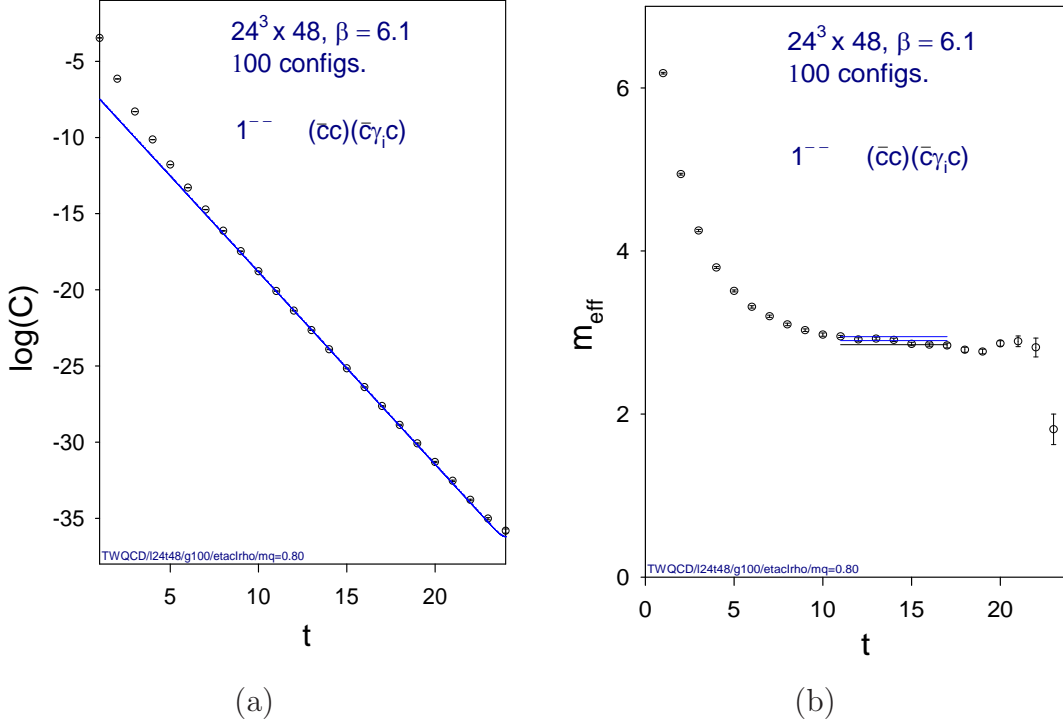


Figure 5: (a) The time-correlation function $C(t)$ of the lowest-lying state of the molecular operator $(\bar{\mathbf{c}}\gamma_i\mathbf{c})(\bar{\mathbf{c}}\mathbf{c})$, on the $24^3 \times 48$ lattice at $\beta = 6.1$. The solid line is the hyperbolic-cosine fit for $t \in [11, 17]$ with $\chi^2/d.o.f. = 0.61$. (b) The effective mass $M_{eff}(t) = \ln[C(t)/C(t+1)]$ of $C(t)$ in Fig. 5a.

$m = c_0 + c_1 m_q$ with $\chi^2/d.o.f. = 0.25$. In the limit $m_q \rightarrow m_u$, it gives $m = 4238(31)$ MeV, which is in good agreement with the mass of $Y(4260)$.

For $m_q = m_s = 0.08a^{-1}$, the time-correlation function and effective mass of M_3 are plotted in Fig. 9. The mass of the lowest-lying state is $4405(31)$ MeV, which is compatible to those obtained from M_1 and M_2 with $m_q = m_s$.

4 The Diquark-Antidiquark Operator

We construct the diquark-antidiquark operator with $J^{PC} = 1^{--}$ as

$$Y_4(x) = \frac{1}{\sqrt{2}} \left\{ [\mathbf{q}^T C \gamma_5 \gamma_i \mathbf{c}]_{xa} [\bar{\mathbf{q}} C \gamma_5 \bar{\mathbf{c}}^T]_{xa} + [\bar{\mathbf{q}} C \gamma_5 \gamma_i^T \bar{\mathbf{c}}^T]_{xa} [\mathbf{q}^T C \gamma_5 \mathbf{c}]_{xa} \right\} \quad (4)$$

where C is the charge conjugation operator satisfying $C\gamma_\mu C^{-1} = -\gamma_\mu^T$ and $(C\gamma_5)^T = -C\gamma_5$. Here the diquark operator $[\mathbf{q}^T \Gamma \mathbf{Q}]_{xa}$ for any Dirac matrix Γ is defined as

$$[\mathbf{q}^T \Gamma \mathbf{Q}]_{xa} \equiv \epsilon_{abc} (\mathbf{q}_{xab} \Gamma_{\alpha\beta} \mathbf{Q}_{x\beta c} - \mathbf{Q}_{xab} \Gamma_{\alpha\beta} \mathbf{q}_{x\beta c}) \quad (5)$$

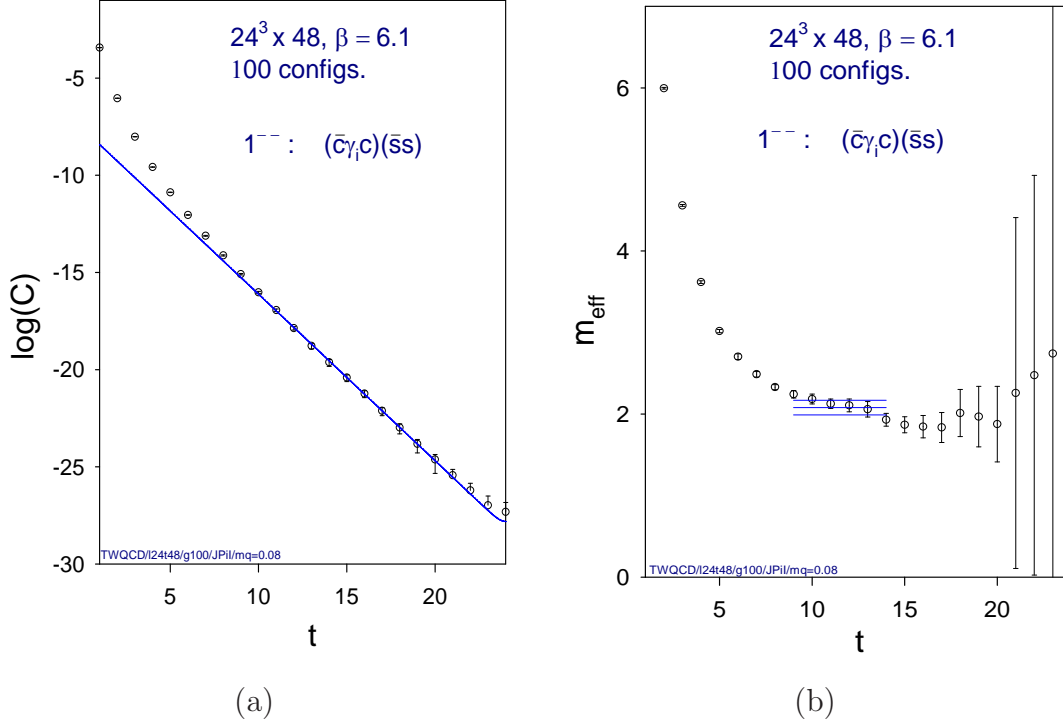


Figure 6: (a) The time-correlation function $C(t)$ of the lowest-lying state of $(\bar{c}\gamma_i\mathbf{c})(\bar{s}s)$, on the $24^3 \times 48$ lattice at $\beta = 6.1$. The solid line is the hyperbolic-cosine fit for $t \in [9, 14]$ with $\chi^2/d.o.f. = 0.56$. (b) The effective mass $M_{eff}(t) = \ln[C(t)/C(t+1)]$ of $C(t)$ in Fig. 6a.

where x , $\{a, b, c\}$ and $\{\alpha, \beta\}$ denote the lattice site, color, and Dirac indices respectively, and ϵ_{abc} is the completely antisymmetric tensor. Thus the diquark (5) transforms like color anti-triplet. For $\Gamma = C\gamma_5$, it transforms like $J^P = 0^+$, while for $\Gamma = C\gamma_5\gamma_i$ ($i = 1, 2, 3$), it transforms like 1^- . In the limit $\mathbf{q} = \mathbf{Q}$, the diquark operator is replaced by $(\mathbf{q}^T\Gamma\mathbf{q})_{xa} \equiv \epsilon_{abc}\mathbf{q}_{xab}\Gamma_{\alpha\beta}\mathbf{q}_{x\beta c}$.

In Fig. 10, the ratio ($R = W_{20}/W_{24}$) of spectral weights of the lowest-lying state extracted from the time-correlation function of Y_4 on the $20^3 \times 40$ and $24^3 \times 48$ lattices is plotted versus the quark mass $m_q a \in [0.03, 0.8]$. Evidently, $R \simeq 1.0$ for $m_q a > 0.05$, in particular, for $m_q = m_s = 0.08a^{-1}$, and $m_q = m_c = 0.8a^{-1}$. This implies that there exist 1^{--} resonances with quark contents $(\mathbf{cc}\bar{c}\bar{c})$ and $(\mathbf{cs}\bar{c}\bar{s})$. On the other hand, as $m_q \rightarrow m_u$, R begins to deviate from 1.0 with large error. This seems to suggest that the diquark-antidiquark operator Y_4 has little overlap with the resonance detected by the molecular operator M_3 as $m_q \rightarrow m_u$. However, it is unclear whether $R \simeq 1$ if one incorporates internal quark loops, and with larger volumes and higher statistics. In the following, we assume this is the case, and obtain its mass by chiral extrapolation.

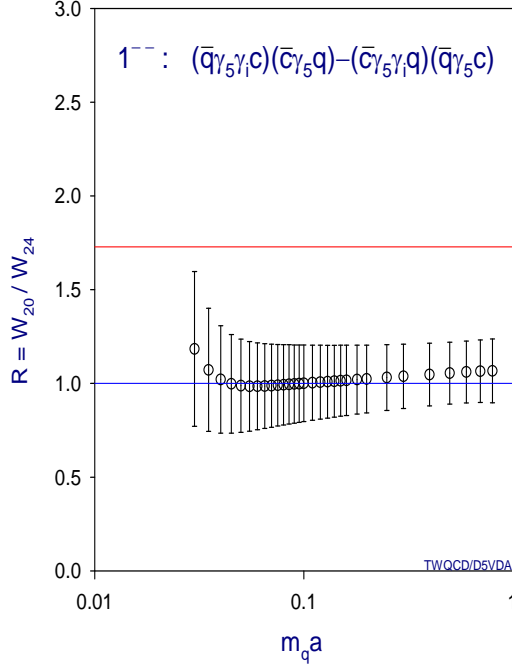


Figure 7: The ratio of spectral weights of the lowest-lying state of the molecular operator M_3 , for $20^3 \times 40$ and $24^3 \times 48$ lattices at $\beta = 6.1$. The upper-horizontal line $R = (24/20)^3 = 1.728$, is the signature of 2-particle scattering state, while the lower-horizontal line $R = 1.0$ is the signature of a resonance.

In Fig. 11, the mass of the lowest-lying state of the diquark-antidiquark operator Y_4 is plotted versus $m_q a$, which can be fitted by the linear function $m = c_0 + c_1 m_q$ with $\chi^2/d.o.f. = 0.49$. In the limit $m_q \rightarrow m_u$, it gives $m = 4267(68)$ MeV, which is in good agreement with the mass of $Y(4260)$.

For $m_q = m_s = 0.08a^{-1}$, and $m_q = m_c = 0.80a^{-1}$, the time-correlation functions and effective masses of the diquark-antidiquark operator are plotted in Fig. 12, and Fig. 13 respectively. The masses of the lowest-lying states are: $m\{[\mathbf{s}^T C \gamma_5 \gamma_i \mathbf{c}][\bar{\mathbf{s}} C \gamma_5 \bar{\mathbf{c}}^T] + [\bar{\mathbf{s}} C \gamma_5 \gamma_i^T \bar{\mathbf{c}}^T][\mathbf{s}^T C \gamma_5 \mathbf{c}]\} = 4449(40)$ MeV with $\chi^2/d.o.f. = 1.03$, and $m\{(\mathbf{c}^T C \gamma_5 \gamma_i \mathbf{c})(\bar{\mathbf{c}} C \gamma_5 \bar{\mathbf{c}}^T) + (\bar{\mathbf{c}} C \gamma_5 \gamma_i^T \bar{\mathbf{c}}^T)(\mathbf{c}^T C \gamma_5 \mathbf{c})\} = 6420(29)$ MeV with $\chi^2/d.o.f. = 0.92$.

Besides Y_4 , we have also constructed other diquark-antidiquark operators, e.g.,

$$\frac{1}{\sqrt{2}} \left\{ [\mathbf{q}^T C \gamma_i \mathbf{c}]_{xa} [\bar{\mathbf{q}} C \bar{\mathbf{c}}^T]_{xa} + [\bar{\mathbf{q}} C \gamma_i^T \bar{\mathbf{c}}^T]_{xa} [\mathbf{q}^T C \mathbf{c}]_{xa} \right\}$$

to see whether they have good overlap with any resonances as $m_q \rightarrow m_u$. However, it turns out that they all behave similar to Y_4 .

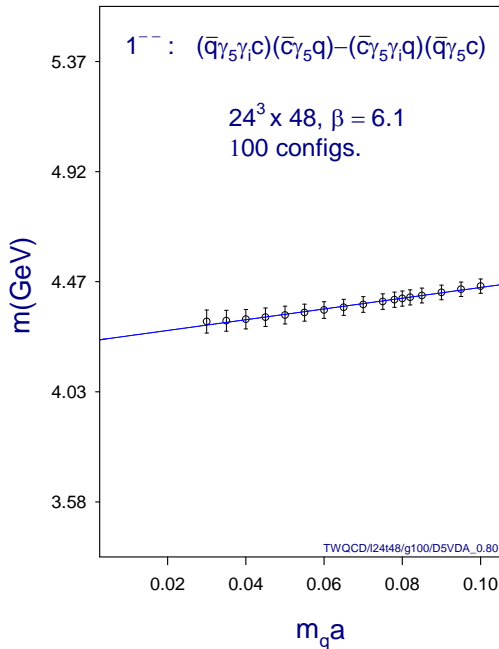


Figure 8: The mass of the lowest-lying state of M_3 versus the quark mass $m_q a$, on the $24^3 \times 48$ lattice at $\beta = 6.1$. The solid line is the linear fit with $\chi^2/d.o.f. = 0.25$.

5 Summary and Discussions

In this paper, we have investigated the mass spectra of several interpolating operators (i.e., the hybrid charmonium $\mathbf{c}\bar{\mathbf{c}}g$, the molecular operators M_1 , M_2 , and M_3 , and the diquark-antidiquark operator Y_4) with $J^{PC} = 1^{--}$, in quenched lattice QCD with exact chiral symmetry. Our results are summarized in Table 1, where in each case, the first error is statistical, and the second one is our estimate of combined systematic uncertainty including those coming from: (i) possible plateaus (fit ranges) with $\chi^2/d.o.f. < 1$; (ii) the uncertainties in the strange quark mass and the charm quark mass; (iii) chiral extrapolation (for the entries containing u/d quarks); and (iv) finite size effects (by comparing results of two lattice sizes). Note that we cannot estimate the discretization error since we have been working with one lattice spacing. Even though lattice QCD with exact chiral symmetry does not have $O(a)$ and $O(ma)$ lattice artifacts, the $O(m^2 a^2)$ effect might turn out to be not negligible for $m_c a = 0.8$.

For the hybrid charmonium ($\epsilon_{ijk}\bar{\mathbf{c}}\gamma_5 F_{jk}\mathbf{c}$), the mass of the lowest-lying state only agrees marginally with the mass of $Y(4260)$. Thus it is unlikely to be identified with $Y(4260)$, even though we cannot rule out such a possibility. Nevertheless, we hope to pin down this problem with a more precise determination

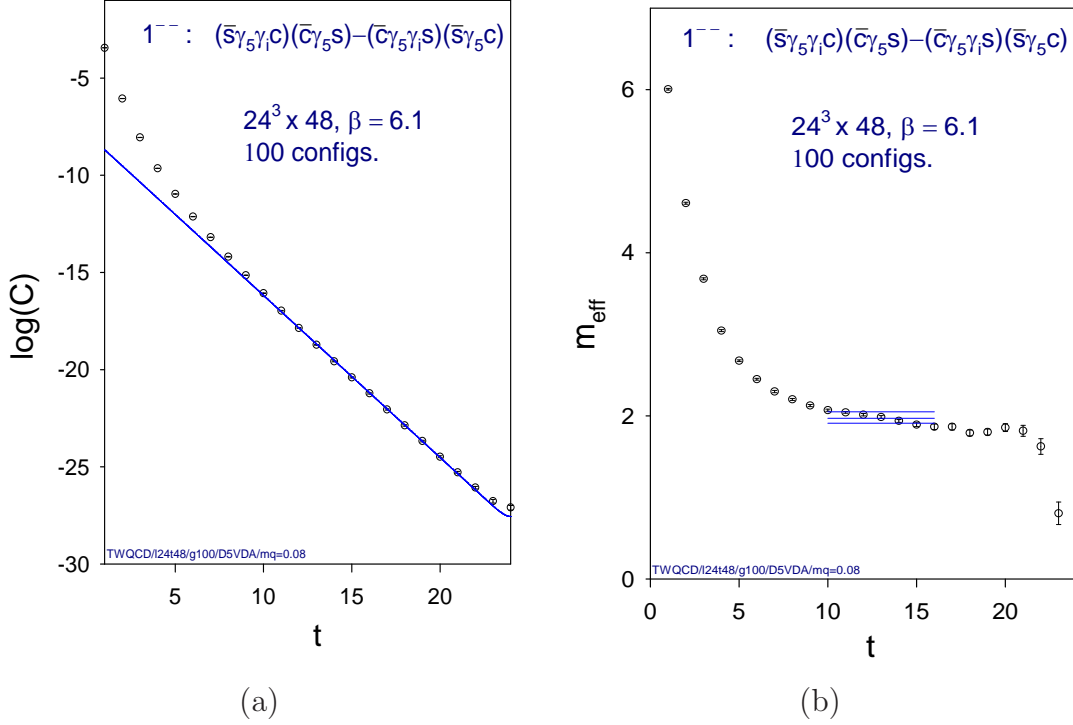


Figure 9: (a) The time-correlation function $C(t)$ of the lowest-lying state of M_3 for $m_q = m_s = 0.08a^{-1}$, on the $24^3 \times 48$ lattice at $\beta = 6.1$. The solid line is the hyperbolic-cosine fit for $t \in [10, 16]$ with $\chi^2/d.o.f. = 1.07$. (b) The effective mass $M_{eff}(t) = \ln[C(t)/C(t+1)]$ of $C(t)$ in Fig. 9a.

of the spectrum of the 1^{--} hybrid charmonium in a future publication.

Evidently, the molecular operator $M_3 \sim \{(\bar{\mathbf{q}}\gamma_5\gamma_i\mathbf{c})(\bar{\mathbf{c}}\gamma_5\mathbf{q}) - (\bar{\mathbf{c}}\gamma_5\gamma_i\mathbf{q})(\bar{\mathbf{q}}\gamma_5\mathbf{c})\}$ detects a resonance ($J^{PC} = 1^{--}$) with mass $4238(31)(57)$ MeV in the limit $m_q \rightarrow m_u$, which is naturally identified with $Y(4260)$. This seems to suggest that $Y(4260)$ is indeed in the spectrum of QCD, with quark content $(\mathbf{c}\bar{\mathbf{u}}\bar{\mathbf{c}})$. Note that we have not studied the excited states of $c\bar{c}$, thus we could not rule out the possibility that $Y(4260)$ might turn out to be one of the excited states of $c\bar{c}$, e.g., $\psi(4^3S_1)$ or $\psi(3^3D_1)$, even though this is very unlikely in view of the widely accepted experimental and theoretical spectrum of $c\bar{c}$.

For the molecular operator $M_1 \sim \{(\bar{\mathbf{q}}\gamma_i\mathbf{c})(\bar{\mathbf{c}}\mathbf{q}) + (\bar{\mathbf{c}}\gamma_i\mathbf{q})(\bar{\mathbf{u}}\mathbf{c})\}$, and the diquark-antidiquark operator $Y_4 \sim \{[\mathbf{q}^T C\gamma_5\gamma_i\mathbf{c}][\bar{\mathbf{q}}C\gamma_5\bar{\mathbf{c}}^T] + [\mathbf{q}^T C\gamma_5\mathbf{c}][\bar{\mathbf{q}}C\gamma_5\gamma_i^T\bar{\mathbf{c}}^T]\}$, they also detect states with masses $4350(69)(88)$ MeV, and $4267(68)(83)$ MeV respectively, in the limit $m_q \rightarrow m_u$. We suspect that they might be the same resonance captured by the molecular operator M_3 . However, we are not sure that these states are resonances since the ratio of spectral weights ($R = W_{20}/W_{24}$) for two different lattice volumes with the same lattice spacing deviates from one (the criterion for a resonance) with large errors as $m_q \rightarrow m_u$.

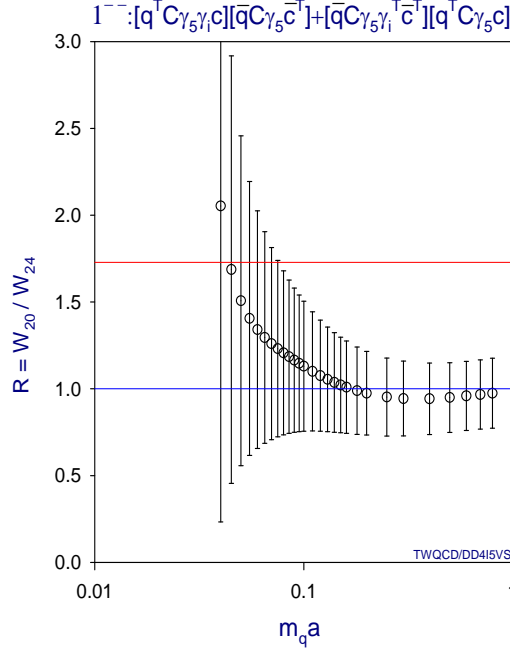


Figure 10: The ratio of spectral weights of the lowest-lying state of diquark-antidiquark operator Y_4 , for $20^3 \times 40$ and $24^3 \times 48$ lattices at $\beta = 6.1$. The upper-horizontal line $R = (24/20)^3 = 1.728$, is the signature of 2-particle scattering state, while the lower-horizontal line $R = 1.0$ is the signature of a resonance.

It is plausible that such a deviation is due to the quenched artifacts which can be evaded if one incorporates internal quark loops.

Now, in the quenched approximation, our results suggest that $Y(4260)$ has a better overlap with the molecular operator M_3 than any other operators discussed in this paper. Whether this implies that $Y(4260)$ behaves more likely as a $D_1 \bar{D}$ molecule than other molecules or diquark-antidiquark meson is subjected to further investigations, especially those incorporating dynamical quarks.

Finally, all molecular and diquark-antidiquark operators with quark fields ($\mathbf{c}\mathbf{s}\bar{\mathbf{c}}\bar{\mathbf{s}}$) detect a resonance around 4450 ± 100 MeV, and those with ($\mathbf{c}\mathbf{c}\bar{\mathbf{c}}\bar{\mathbf{c}}$) detect a resonance around 6400 ± 50 MeV. These serve as predictions of lattice QCD with exact chiral symmetry.

Acknowledgement

This work was supported in part by the National Science Council, Republic of China, under the Grant No. NSC94-2112-M002-016 (T.W.C.), and

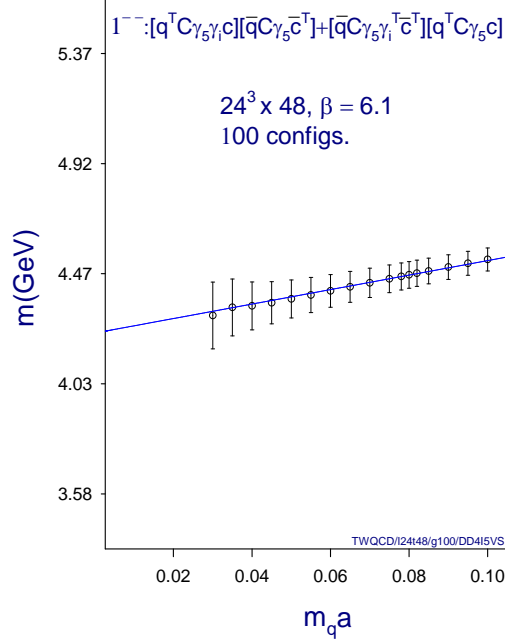


Figure 11: The mass of the lowest-lying state of the diquark-antidiquark operator Y_4 versus the quark mass $m_q a$, on the $24^3 \times 48$ lattice at $\beta = 6.1$. The solid line is the linear fit with $\chi^2/d.o.f. = 0.49$.

Grant No. NSC94-2119-M239-001 (T.H.H.), and by National Center for High Performance Computation at Hsinchu. T.W.C. would like to thank the kind hospitality of Yukawa Institute for Theoretical Physics at Kyoto University, where the final version of this paper was prepared during the YITP workshop "Actions and symmetries in lattice gauge theory" (YITP-W-05-25).

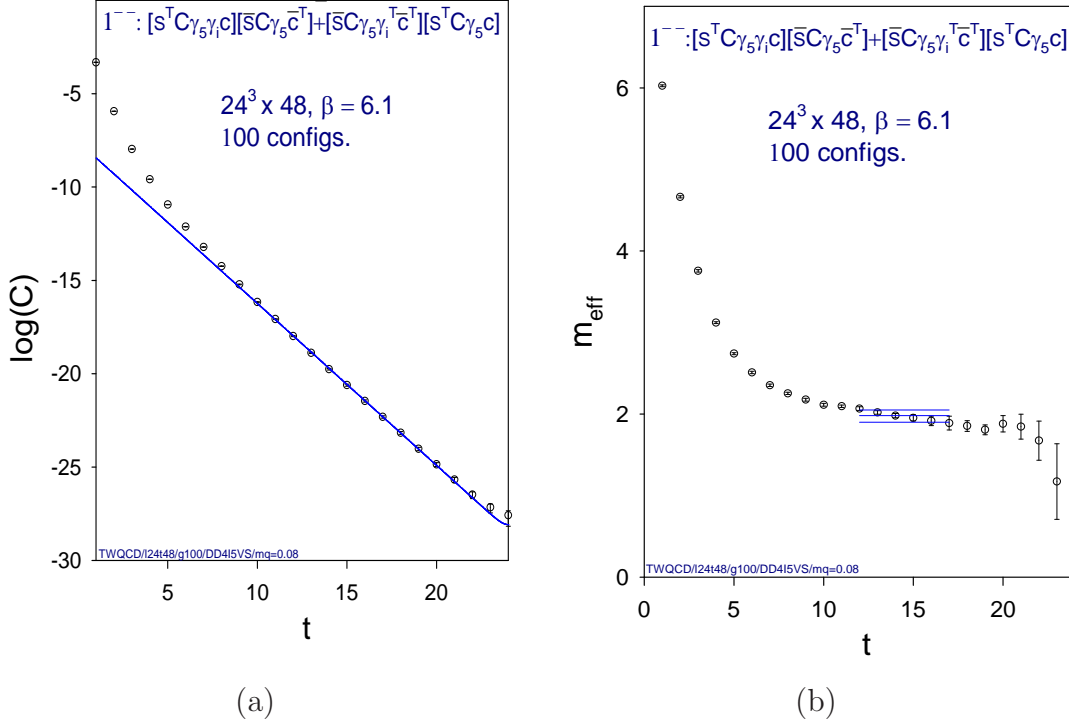


Figure 12: (a) The time-correlation function $C(t)$ of the lowest-lying state of Y_4 for $m_q = m_s = 0.08a^{-1}$, on the $24^3 \times 48$ lattice at $\beta = 6.1$. The solid line is the hyperbolic-cosine fit for $t \in [12, 17]$ with $\chi^2/d.o.f. = 1.03$. (b) The effective mass $M_{eff}(t) = \ln[C(t)/C(t+1)]$ of $C(t)$ in Fig. 12a.

References

- [1] B. Aubert *et al.* [BABAR Collaboration], Phys. Rev. Lett. **95**, 142001 (2005)
- [2] S. L. Zhu, Phys. Lett. B **625**, 212 (2005)
- [3] F. E. Close and P. R. Page, Phys. Lett. B **628**, 215 (2005)
- [4] L. Maiani, V. Riquer, F. Piccinini and A. D. Polosa, Phys. Rev. D **72**, 031502 (2005); R. L. Jaffe, Phys. Rev. D **15**, 267 (1977).
- [5] X. Liu, X. Q. Zeng and X. Q. Li, Phys. Rev. D **72**, 054023 (2005)
- [6] D. B. Kaplan, Phys. Lett. B **288**, 342 (1992); Nucl. Phys. Proc. Suppl. **30**, 597 (1993).
- [7] R. Narayanan and H. Neuberger, Nucl. Phys. B **443**, 305 (1995)
- [8] H. Neuberger, Phys. Lett. B **417**, 141 (1998)

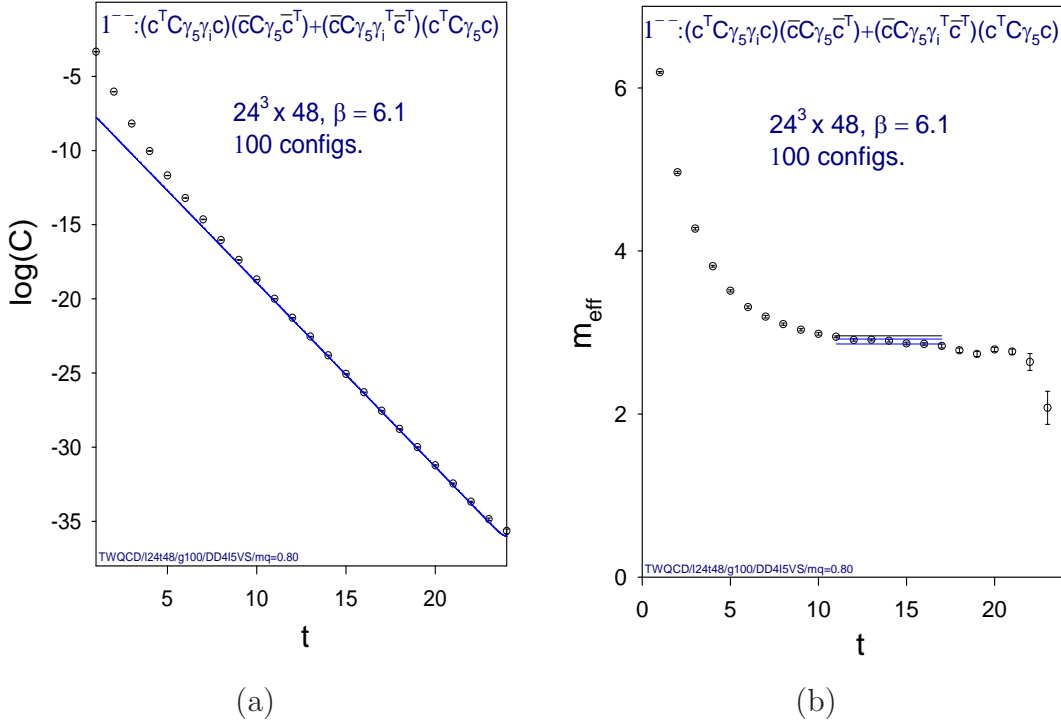


Figure 13: (a) The time-correlation function $C(t)$ of the lowest-lying state of Y_4 for $m_q = m_c = 0.80a^{-1}$, on the $24^3 \times 48$ lattice at $\beta = 6.1$. The solid line is the hyperbolic-cosine fit for $t \in [11, 17]$ with $\chi^2/d.o.f. = 0.92$. (b) The effective mass $M_{eff}(t) = \ln[C(t)/C(t+1)]$ of $C(t)$ in Fig. 13a.

- [9] P. H. Ginsparg and K. G. Wilson, Phys. Rev. D **25**, 2649 (1982)
- [10] T. W. Chiu, Phys. Rev. Lett. **90**, 071601 (2003); Phys. Lett. B **552**, 97 (2003); hep-lat/0303008; Nucl. Phys. Proc. Suppl. **129**, 135 (2004).
- [11] T. W. Chiu and T. H. Hsieh, Nucl. Phys. A **755**, 471 (2005); T. W. Chiu, T. H. Hsieh, J. Y. Lee, P. H. Liu and H. J. Chang, Phys. Lett. B **624**, 31 (2005)
- [12] T. W. Chiu and T. H. Hsieh, Nucl. Phys. B **673**, 217 (2003); Phys. Rev. D **72**, 034505 (2005)
- [13] Y. Iwasaki *et al.* [QCDPAX Collaboration], Phys. Rev. D **53**, 6443 (1996)

Operator	Mass (MeV)	Resonance/Scattering
$\epsilon_{ijk}\bar{\mathbf{c}}\gamma_5 F_{jk}\mathbf{c}$	4501(178)(215)	Resonance
$\frac{1}{\sqrt{2}}[(\bar{\mathbf{u}}\gamma_i\mathbf{c})(\bar{\mathbf{c}}\mathbf{u}) + (\bar{\mathbf{c}}\gamma_i\mathbf{u})(\bar{\mathbf{u}}\mathbf{c})]$	4350(69)(88)	Resonance ?
$\frac{1}{\sqrt{2}}[(\bar{\mathbf{s}}\gamma_i\mathbf{c})(\bar{\mathbf{c}}\mathbf{s}) + (\bar{\mathbf{c}}\gamma_i\mathbf{s})(\bar{\mathbf{s}}\mathbf{c})]$	4546(30)(61)	Resonance
$\frac{1}{\sqrt{2}}[(\bar{\mathbf{u}}\gamma_5\gamma_i\mathbf{c})(\bar{\mathbf{c}}\gamma_5\mathbf{u}) - (\bar{\mathbf{c}}\gamma_5\gamma_i\mathbf{u})(\bar{\mathbf{u}}\gamma_5\mathbf{c})]$	4238(31)(57)	Resonance
$\frac{1}{\sqrt{2}}[(\bar{\mathbf{s}}\gamma_5\gamma_i\mathbf{c})(\bar{\mathbf{c}}\gamma_5\mathbf{s}) - (\bar{\mathbf{c}}\gamma_5\gamma_i\mathbf{s})(\bar{\mathbf{s}}\gamma_5\mathbf{c})]$	4405(31)(44)	Resonance
$(\bar{\mathbf{c}}\gamma_i\mathbf{c})(\bar{\mathbf{s}}\mathbf{s})$	4581(96)(115)	Resonance
$(\bar{\mathbf{c}}\gamma_i\mathbf{c})(\bar{\mathbf{c}}\mathbf{c})$	6411(25)(43)	Resonance
$\frac{1}{\sqrt{2}}\left\{[\mathbf{u}^T C\gamma_5\gamma_i\mathbf{c}][\bar{\mathbf{u}}C\gamma_5\bar{\mathbf{c}}^T] + [\mathbf{u}^T C\gamma_5\mathbf{c}][\bar{\mathbf{u}}C\gamma_5\gamma_i^T\bar{\mathbf{c}}^T]\right\}$	4267(68)(83)	Resonance ?
$\frac{1}{\sqrt{2}}\left\{[\mathbf{s}^T C\gamma_5\gamma_i\mathbf{c}][\bar{\mathbf{s}}C\gamma_5\bar{\mathbf{c}}^T] + [\mathbf{s}^T C\gamma_5\mathbf{c}][\bar{\mathbf{s}}C\gamma_5\gamma_i^T\bar{\mathbf{c}}^T]\right\}$	4449(40)(55)	Resonance
$\frac{1}{\sqrt{2}}\left\{(\mathbf{c}^T C\gamma_5\gamma_i\mathbf{c})(\bar{\mathbf{c}}C\gamma_5\bar{\mathbf{c}}^T) + (\mathbf{c}^T C\gamma_5\mathbf{c})(\bar{\mathbf{c}}C\gamma_5\gamma_i^T\bar{\mathbf{c}}^T)\right\}$	6420(29)(32)	Resonance

Table 1: Mass spectra of hybrid charmonium, molecules, and diquark-antidiquark operators with $J^{PC} = 1^{--}$.